Developing Robust Early Measures of Tibiofemoral Joint Health Following ACL Reconstruction

Evan Larson, Tyce C. Marquez, Donald D. Anderson

University of Iowa, Iowa City, Iowa

larsonev@grinnell.edu

INTRODUCTION: Post-traumatic osteoarthritis (PTOA) after ACL reconstruction (ACLR) is common, with roughly 50% of individuals having symptoms 10 to 20 years later [1]. Traditional diagnostic 2D radiographic imaging modalities, while effective for later-stage diagnosis, often fall short in capturing more subtle alterations in joint health marking early PTOA [2]. Recent reports link the load-bearing pose of the knee following ACLR to early compositional MRI changes in articular cartilage consistent with PTOA [3]. Weight bearing CT (WBCT) offers potential to leverage this finding for more robust early diagnostic capabilities because it is inherently 3D in nature, images the joint in a functional load bearing pose, and captures bony anatomy with high fidelity. Two logical targets for measures of joint health are 3D joint space width (JSW) and bony articular congruence. The objective of this study was to begin developing more robust WBCT-enabled measures of tibiofemoral joint health for diagnosis of OA early after ACLR.

METHODS: Thirty-six subjects (13M/23F, age: 22.07±8.66 years) with a unilateral isolated partial or complete ACL tear reconstructed by one of three surgeons were recruited to participate in this IRB-approved study. Bilateral knee WBCT scans were acquired in a semi-flexed (~30°) pose 3.3±0.6 months post ACLR. A fully automated method [4] was used to compute 3D JSW from WBCT and to segment the femoral condyles and tibial plateau for evaluation of congruence. A statistical shape model (SSM) was created for the medial compartment from 3D JSW maps where the JSW<10 mm using the open-source software ShapeWorks. The JSW threshold of 10 mm was chosen to provide a reasonable approximation of the entire articular surface available for contact. To quantify bony congruence, the congruence index (CI) [5] of the medial compartment was computed from principal curvatures of the segmented bone surfaces in MeshLab. All JSW and congruence maps were aligned to the SSM using a non-rigid iterative closest point (ICP) algorithm to allow for collective data analysis. Comparisons were made between ACLR and intact contralateral knees, in aggregate.

RESULTS: The automated analysis of the medial compartment measured a 3D JSW of 5.6±0.6 mm (mean±SD) across all knees. ACLR knees had a JSW of 5.6±0.6 mm, compared to the intact knee JSW of 5.5±0.7 mm (Figure 1). For CI, both groups displayed an average of 0.3±0.1 mm^{-1}, with the ACLR group at .26±.09 mm^{-1} and the intact group at 0.25±.11 mm^{-1}.

DISCUSSION: Both JSW and CI depicted similar distributions between ACLR and intact groups 3 months post-ACLR (Figure 2). The similar distributions indicate that there are no differences at the 3-month post-op timepoint. Although the overall distributions are similar for both JSW and CI, the mean aligned 3D maps of JSW and CI data demonstrate areas of possible importance in further longitudinal studies. Such areas include the tibial spine and locations of smallest JSW values in the medial-central portion of the medial compartment. While data are not shown here, females had substantially less JSW than males, something that will need to be included in analytical models. This study is ongoing, with subjects returning for 1-year post-op visits, a timepoint in which changes are more likely to be observable.

SIGNIFICANCE/CLINICAL RELEVANCE: Establishment of WBCT-based 3D diagnostic imaging markers such as JSW and CI can help provide early detection of PTOA post ACLR and lead to more effective clinical longitudinal studies.
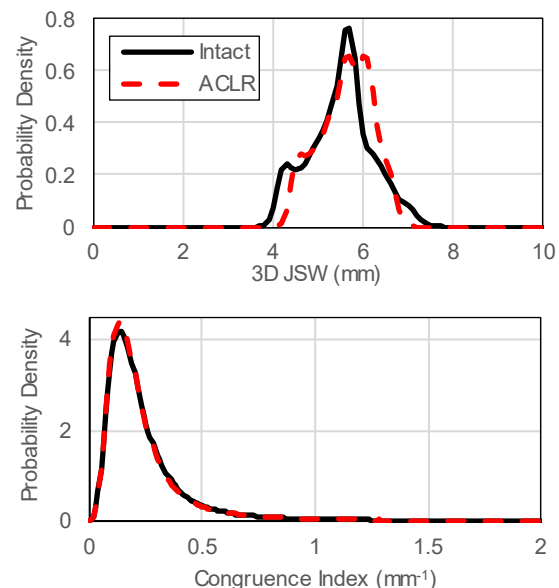
REFERENCES: [1] Lohmander LS, et al. 2007. Am J Sports Med 35(10):1756-69. [2] Chang JC et al. 2017. J Orthop Res 35:464-85. [3] Lansdown DA, et al. 2020. J Orthop Res 38(6):1289-95. [4] McFadden EJ, et al. 2022. OA&Cartilage 30(S1):S284-5. [5] Ateshian GA et al. 1992. J Biomech 25(6):591-607.

IMAGES AND TABLES:
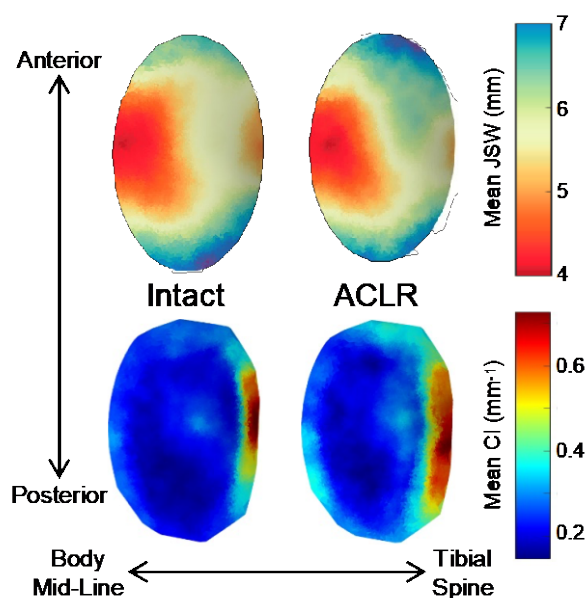
Figure 1: (Top) Average JSW models on mean SSM. (Bottom) Average CI models on mean SSM surface.

Figure 2: (Top) JSW Distribution. (Bottom) CI Distribution.